Gravitational waves from a black hole orbiting in a wormhole geometry

James B. Dent,[1,*] William E. Gabella,[2,†] Kelly Holley-Bockelmann,[2,‡] and Thomas W. Kephart[2,§]

[1]*Department of Physics, Sam Houston State University, Huntsville, Texas 77341, USA*

[2]*Department of Physics and Astronomy, Vanderbilt University, Nashville, Tennessee 37235, USA*

(Received 30 July 2020; revised 4 December 2020; accepted 13 July 2021; published 13 August 2021)

Current ground-based gravitational wave detectors are tuned to observe compact object mergers from stellar mass black holes and neutron stars; ~50 such events have been published to date. More exotic compact objects may exist, collisions of which would also generate copious gravitational waves. We model a stellar mass black hole inspiral into a stable, nonspinning, traversable wormhole, and find a characteristic waveform—an *antichirp* and/or *burst*—as the black hole outspirals into our region of the Universe. This is a characteristic signature which can be useful in wormhole searches in gravitational wave data or used to constrain wormhole geometries.

DOI: 10.1103/PhysRevD.104.044030

I. INTRODUCTION

The discovery of black hole-black hole (BH-BH) [1], black hole-neutron star (BH-NS) [2], and NS-NS mergers [3] has launched gravitational wave (GW) astronomy, and unveiled a class of stellar origin BHs in the 30–60 $M_\odot$ range [4]. Beyond inspiraling binary BH and NS systems, GWs can detect a variety of objects ranging from cosmic defects [5] to exoplanets [6]. In exotic compact objects, such as wormholes (WHs) [7,8] inspirals may also be detectable; see Fig. 1. Finding these other source types depends on detecting a signal that is observationally distinguishable from other inspiraling binary systems [9].

Prior investigations of WH binaries focused on the quasinormal modes produced during the ringdown, and the subsequent echo produced in a horizonless geometry (see for example [9–16]). It was conjectured that the ringdown signal could probe the existence of a horizon. However, these studies conclude that ringdown is independent of the existence of a horizon as long as the compact object has a light ring, i.e., an unstable circular orbit. Further studies of echoes from compact objects, including Bose stars and gravastars, can be found in [11,12]. One case in which echoes could still depend on the existence of a horizon is for a Schwarzschild thin-shell wormhole—in this case the throat at $3M$ and the light ring are formally at the same distance, which could, in principle, reveal the lack of horizon via late-time ringdown echos. Further details can be found in [9,10] and references therein, and citations thereof. Hence, this marginal case is particularly interesting to investigate in great detail.

[*]jbdent@shsu.edu
[†]b.gabella@vanderbilt.edu
[‡]k.holley@vanderbilt.edu
[§]tom.kephart@gmail.com

Here, we argue that a BH spiraling into and through a traversable WH could generate a very distinct observational signature well before ringdown. We follow a BH orbit as it proceeds through the WH, outspirals into another spacetime, and then (in the case of an object gravitationally bound to the WH) back into ours. This will produce a gap within the postchirp GW signal when the object passes through the throat. The overall waveform of such a source would be quite complex, with chirp, gap, and possible antichirp cycles resulting from the GW emission. Alternatively, we could observe only a burst or an antichirp if the BH first emerges into our spacetime. This work explores a simple traversable WH with these signature types.

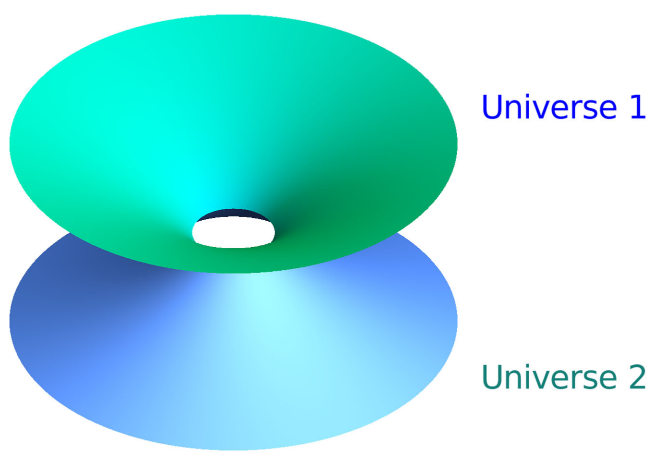

FIG. 1. We show an embedding diagram depicting a wormhole that connects two different universes, where the upper branch is Universe 1 and the lower is Universe 2. The throat is a thin shell of "exotic material" and there is no spacetime within the "hole."

Our purpose in the present work is to study gravitational waves from the inspiral of the simplest possible wormhole with the simplest possible orbits, i.e., quasicircular, to lay down a baseline signal. This will facilitate comparison with the equivalent simple BH-BH interaction, and further provides a foundation with which to compare with other merger signals with a variety of compact horizonless objects on less idealized orbits. Specifically, we will not consider echoes or other modifications of the GW signals, although we will comment on how we expect our results could be modified if such effects were included. Hence our results lay the basis of BH-WH gravitational waveforms, around which perturbations can be studied; we intend to explore some of these possibilities in the future.

II. WORMHOLE CONSTRUCTION

Consider a traversable Lorentzian WH [17–19] of apparent mass M_{WH} surgically constructed from two Schwarzschild BH spacetimes with a BH of mass M_{BH} falling into the WH, where we require $M_{\mathrm{BH}} < M_{\mathrm{WH}}$. For technical reasons (see below) we take the mass ratio $M_{\mathrm{WH}}/M_{\mathrm{BH}} \gtrsim O(10)$. This range could be extended to larger mass ratios at the expense of a longer simulation, or to smaller mass ratios with further theoretical analysis and more careful approximations.

We review the simplest Schwarzschild wormhole [20,21]. Starting with two Schwarzschild BHs of equivalent ADM mass $M = M_{\mathrm{WH}}$ [22], the line element is

$$ds^2 = -\left(1 - \frac{2M}{r}\right)dt^2 + \frac{dr^2}{(1 - \frac{2M}{r})} + r^2(d\theta^2 + \sin^2\theta d\varphi^2). \tag{1}$$

We excise a sphere of radius a that is outside and concentric with the nominal event horizon at $2M$ from both BHs, and identify the two boundaries, ensuring the manifold remains orientable. Finally we distribute exotic energy density at the boundary to satisfy the junction formalism [23] for Einstein equations everywhere.

Converting to Gaussian normal coordinates for the static case, the metric is

$$\begin{aligned} ds^2 = &-\left(1 - \frac{2M_{\mathrm{WH}}}{R(\eta)}\right)dt^2 + d\eta^2 \\ &+ R(\eta)^2(d\theta^2 + \sin^2\theta d\varphi^2), \end{aligned} \tag{2}$$

where η is the proper radius and $R(\eta)$ satisfies $R/\eta = \pm\sqrt{1 - 2M_{\mathrm{WH}}/R}$.

The WH is composed of three regions: two Schwarzschild BH exteriors, where the stress-energy tensor is known (denoted here as *Universe 1* and *Universe 2*), and the *boundary*, where the surface stress-energy tensor is determined by assumption or experiment. η is positive in Universe 1, negative in Universe 2, and zero on the boundary or throat.

The stress-energy tensor is

$$T^{\mu\nu} = S^{\mu\nu} \cdot \delta(\eta) + T_1^{\mu\nu} \cdot \Theta(\eta) + T_2^{\mu\nu} \cdot \Theta(-\eta), \tag{3}$$

where $\Theta(\eta)$ is a step function. For Einstein gravity, matter on the WH throat invariably violates energy conditions [24], depending on its equation of state, possibly leading to instabilities [20,21,25,26]. The linear stability analysis of [27] showed that exotic matter, or exotic physics, is required for a stable positive mass wormhole. However, examples such as a Casimir vacuum or a variable equation of state [28] may allow for a stable positive mass configuration. As the focus of the present work is on the GW signature from a wormhole geometry, we remain agnostic to the choice of microphysics of any throat matter. A more thorough analysis of energy condition violations [29–31] by wormholes was carried out in [32], where they showed that spherically symmetric wormholes, of which Schwarzschild is a special case, violate the Average Null Energy Condition (ANEC), but those violations can be made arbitrarily small. They concluded that ANEC violations for wormholes can be arranged to be no worse than the quantum violations of ANEC for the area increase theorem required by Hawking radiation. Hence the instability of the exotic matter required for a wormhole could be likewise reduced.

As an example of a Schwarzschild WH, we envision material with equation of state $\sigma = \tau$ on the throat, where σ is a negative surface energy density and τ is a negative pressure, i.e., surface tension. While this equation of state is similar to a classical negative energy density membrane, the matter need not be a membrane; it could consist of particles with attractive interactions. Hence, the stress-energy tensor on the throat is $S^i{}_j = \mathrm{diag}(\sigma, -\tau, -\tau)$. The Einstein equations on the throat lead to a throat radius $a = 3M = 3M_{\mathrm{WH}}$ [20], on identifying the mass M with the effective WH mass.

Now consider a BH falling into a WH of the type just described. Since the WH looks just like a BH outside the radius $3M_{\mathrm{WH}}$, the infall is indistinguishable from a BH-BH merger to an observer in Universe 1 until the BH reaches that radius. However, at that point the BH encounters the material on the throat. The interaction may be rather benign or not, depending on the material properties. We assume the simplest possibility: that there are only gravitational interactions between the throat matter and the infalling BH, and that the throat matter is made up of particles confined to the throat, but are otherwise free to move. Since the throat matter has negative energy density, it is repelled by the positive mass BH, causing it to simply move aside as the BH passes through. After the BH transit, the throat matter will redistribute itself in its original state with minimal temporary disruption of the WH. The BH then passes through and spirals out the other end of the WH into Universe 2. Depending on the radial component of the BH's momentum, the BH can either move off to infinity in Universe 2 or be trapped in a series of transits through the WH.

What are the observational expectations in the above scenario? We assume the mouths of the WH in Universe 1 and Universe 2 are well separated so that an observed GW signal in Universe 1 will not overlap with a signal associated with the emergence of the BH in Universe 2, unless a shortcut is taken through the WH. As seen by an observer in Universe 1, the initial inspiral of the BH would exhibit the familiar features of a typical BH-BH inspiral. It is important to note that the standard signal from the inspiral may be accompanied by backscattering of radiation due to the excitation of additional oscillatory modes depending on the nature of the throat; gravastars, for example, are horizonless objects which have been shown to produce such features [33,34]. Couplings to additional scalar fields in extensions to general relativity (GR) as described in [35], may also excite additional modes, potentially producing substantive GW signals. We reserve these additional effects for future parameter studies. At some point, the BH passes through the throat into Universe 2 and the GW signature in Universe 1 fades quickly as the BH radiates predominantly into Universe 2. An observer in Universe 2 sees a very strong signal that decreases in amplitude and frequency, an *antichirp*, until the BH reaches apogee and falls back into the WH. The frequency reaches a maximum again at the throat as it returns to Universe 1, and the process repeats—with chirps resulting from the inspirals and antichirps from outspirals. With sufficient radial velocity, the GW emission near the apogee will be undetectable, reminiscent of *zoom-whirl* orbits seen in extreme mass ratio inspirals [36]. If the BH is bound to the WH, it eventually settles near the throat with consequences depending on the properties of the unknown exotic matter.

As mentioned in the Introduction, another discrepancy from the standard expectations of a BH-BH merger waveform could occur during the postcoalescence ringdown phase. It has been suggested that a horizonless object such as a wormhole can produce modified signals including echoes [11,12], or enhancement of modes associated with couplings to scalar fields as seen in some beyond GR scenarios (see [35], for example).

Antichirps and gaps in the GW frequency spectrum are distinctive signatures that could be used to constrain the number of WHs in our Universe. These GW signatures could be searched for in existing Laser Interferometer Gravitational Wave Observatory (LIGO) data by comparing with antichirplike waveforms. While these constraints would only apply to a limited range of WH types—namely traversable ones—they could still have astrophysical and cosmological implications.

There are other signals, such as superradiance [37], which could display some similarities to the antichirp signal. However, characteristics such as monochromatic waveforms [38], possible postmerger effects [39,40], and angular momentum loss due to superradiance are ways to differentiate between a WH-BH inspiral and these scenarios. In addition, a key feature of the WH-BH inspiral is the repetition of the antichirp signal from several orbital passes through the wormhole.

In the example that follows, we let $M_{\mathrm{BH}} = 5\ M_{\odot}$ and $M_{\mathrm{WH}} = 200\ M_{\odot}$. The throat is at radius $a = 3M_{\mathrm{WH}} = 60R_{s,\mathrm{BH}}$, where $R_{s,\mathrm{BH}}$ is the Schwarzschild BH radius, leading to a cross-sectional area of the WH throat that is roughly 3600 times larger than the area of the BH horizon. Thus it is reasonable to consider a BH passing through the WH throat as a perturbation of the WH when the interaction with the exotic matter is not too strong; this would be the case if the exotic matter is evenly distributed particles on the throat that only interact gravitationally with the BH ($\sigma < 0$). Under these constraints, the traversing BH is not expected to accrete exotic matter, and indeed repels it. Naturally, if exotic matter has different constraints, or reacts to additional forces, BH accretion must be reconsidered.

III. ORBITAL DYNAMICS AND GRAVITATIONAL WAVES

There is a rich suite of possible WH-BH orbits, even in the relatively simple regime in which $M_{\mathrm{WH}} \gg M_{\mathrm{BH}}$. For a Schwarzschild-like WH, the throat radius is at 1.5 times the Schwarzschild radius for an equivalent BH—we stress, though, that the WH is horizonless. For the unequal masses of our example, the BH-exotic matter interaction at the throat is a minor perturbation to the matter and geometry of the system, which facilitates a post-Newtonian treatment of the dynamics. We find that a bound BH will move through the WH many times in a damped oscillation, emitting energy into GWs on each side of the throat. This results in the BH orbit decaying and settling on the WH throat. Here we explore noneccentric orbits, which is the expected situation for binary systems due to the circularizing effects of the radiation reaction on the system [41], but one could extend this approach to systems with eccentricity developed, for example, via the Kozai-Lidov mechanism [42,43].

In our example we consider what would be a circular, bound orbit (BO) in our Universe if there were no gravitational radiation [44]. Including gravitational radiation, the orbit loses energy and spirals into the WH throat, continues damped oscillations between spacetime regions, a so-called two-world bound (TWB) orbit, until it eventually settles to the throat. Following Diemer and Smolarek [45], orbits are categorized as BO: orbital motion is around the throat of the WH, never passing to the other side; TWB: orbits passing through the throat of the WH at least once; *two-world escape:* orbits with enough energy that they go from radial infinity, pass through the WH, and to radial infinity on the other side; and *escape orbits* which come in from radial infinity, swing around the WH and escape back out to radial infinity staying in a single universe. In future work, we will consider additional trajectory topologies and their subsequent GW signatures.

To model the dynamics, we use the ARCHAIN code [46,47] for integrating the two-body equations of motion up to 3.5 post-Newtonian (PN) order, including gravitational radiation at 2.5 PN. We treat the WH as a large mass with a smaller BH orbiting it. Neither object is spinning. One might be concerned with following the trajectory up to and through the WH, as PN approximations are thought to break down close to BH-BH mergers [48]. However, here, the orbital inspiral stops effectively at $1.5R_{s,\mathrm{WH}}$, as it traverses to a new universe, which mitigates some of the mismatch between a more realistic NR and a PN-calculated treatment [49–51]. In the outermost orbit shown in Fig. 3, the maximum velocity is entering the throat the first time and is 0.43 in units of the speed of light.

Our 40∶1 mass ratio makes the problem computationally difficult but not impossible for current numerical relativity simulations which have calculated ratios as high as 128∶1 and 100∶1 in certain cases [52,53] and more generally for mass ratios of 18.9∶1 [54] and 15∶1 [55]. These cases are still computationally expensive. This is an active area of research, with one recent study comparing numerical relativity at a 10∶1 ratio with the small mass ratio expansion to extend NR to ratios around 1000∶1 [56].

Table I presents initial conditions for our near-circular orbit. Included are the WH and BH center-of-mass positions and velocities in the xy plane for the starting position near $x_{\mathrm{BH}} \sim 20$ (in units of $R_{s,\mathrm{WH}} = 2M_{\mathrm{WH}}$) which is integrated with a coarse step size. Positions and velocities are taken from that trajectory near $x_{\mathrm{BH}} \sim 7$ as the initial conditions to calculate a more finely resolved trajectory. All motion is in the xy plane, and neither the WH nor the BH has spin.

We use units such that $2M_{\mathrm{WH}} = R_{s,\mathrm{WH}} = 1$, the gravitational constant $G = 1$, and the speed of light $c = 1$. In SI units, the unit of length is $U_l = 5.9065 \times 10^5$ m, of mass $U_m = 400\ M_\odot = 7.9536 \times 10^{32}$ kg, and of time is $U_t = 1.9702 \times 10^{-3}$ s.

Figure 2 shows the initial inspiral and four passes through the throat of the WH in an embedding diagram, following that of [45]. The upper half of the hyperboloid is Universe 1, which contains the initial position, and the lower half is Universe 2. Trajectories in Universe 1 are solid lines; those in Universe 2 are dashed.

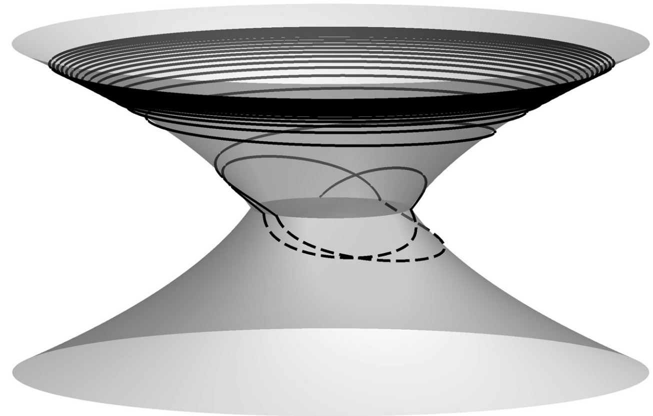

FIG. 2. We show the embedding diagram for an orbit following Diemer and Smolarek [45] for a BH with mass 5 $M_\odot$ around and through a WH with an effective mass 200 $M_\odot$. Without GWs this would be a bound, circular orbit in Universe 1 (top half). The initial position is at the top of the hyperboloid; the inspiral of the BH can be seen. As it passes the throat into Universe 2 (bottom half), we indicate orbits in Universe 2 with dashed lines. Five "passes" or "petals" are shown, three in Universe 1 and two (dashed) in Universe 2.

The orbital piece shown in Fig. 3 that corresponds to Universe 1 is used to calculate the gravitational strain in Universe 1, as shown in Fig. 4. The orbit shows that the BH will asymptotically settle on the throat of the WH as energy and angular momentum are radiated away; presumably this would also hold for any normal matter. The WH could potentially collect a set of compact objects on its throat, the observational and theoretical consequences of which have yet to be explored. Figure 5 displays the same gravitational wave strain at late times to better show the gaps in the waveform.

We calculate the GWs using the mass quadrupole formula given in [57] [see Eq. (3.72)] treating the two bodies as point particles. Since the strain $h \sim d^2 Q_{ij}/dt^2$, where Q_{ij} is the mass quadrupole moment of the binary, we smooth the orbits using a fifth-order spline to have a smooth second derivative. In Fig. 5, the spikes at the boundaries of the bursts of radiation come from the plunge of the black hole into the throat. To avoid numerical discontinuities at the throat, the orbits were calculated into the throat to be continuous there. Then the GW waveform

TABLE I. Initial conditions for the 200 $M_\odot$ WH and 5 $M_\odot$ BH, showing the center-of-mass positions and velocities in the xy plane. The first row denotes the initial conditions for a coarsely integrated trajectory used to find the position and velocities in the second row, which are used to start the finely integrated trajectory used for the GW calculation.

x_{WH}	y_{WH}	$v_{x,\mathrm{WH}}$	$v_{y,\mathrm{WH}}$	x_{BH}	y_{BH}	$v_{x,\mathrm{BH}}$	$v_{y,\mathrm{BH}}$	Step size
−0.4878	0	0	-3.7611×10^{-3}	19.512	0	0	0.15045	4.0
−0.17973	3.4144×10^{-4}	-7.3384×10^{-6}	-5.8446×10^{-3}	7.1894	−0.013658	2.9353×10^{-4}	0.23379	0.0001

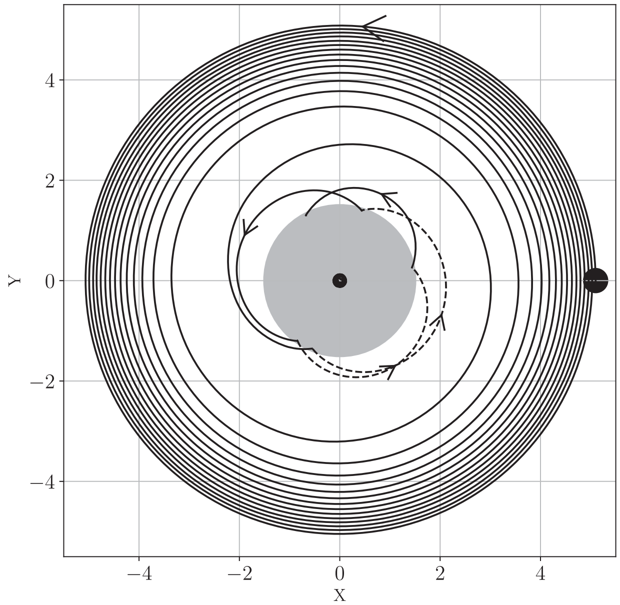

FIG. 3. We show the orbits of the BH in Fig. 2 from above. The orbit starts in Universe 1 and traverses to 2, then back in 1, etc. The black circle marks the initial position and the circulation of the orbits are counterclockwise. The solid gray circle is approximately the WH throat—the center of the WH executes the small orbit indicated by the black dot around the origin. Orbits in Universe 2 are shown dashed.

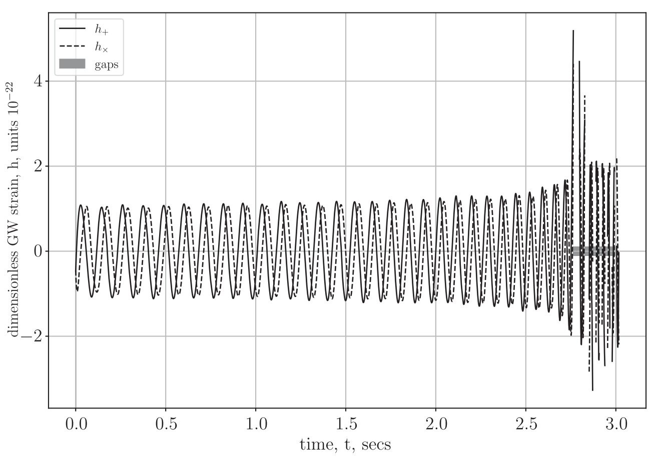

FIG. 4. Shown is the dimensionless gravitational strain measured for the WH-BH binary shown in Fig. 3 at a distance of 500 Mpc and at $\varphi = \pi/4$ and $\theta = \pi/4$ relative to the binary orbital plane. The WH mass is 200 $M_\odot$ and the BH is 5 $M_\odot$. The estimated GW frequency of this example is approximately 9 Hz near $t = 0$.

was calculated, and truncated at the time the BH enters the throat at $3M_{\mathrm{WH}}$. In a fuller model, we expect strong GWs from this passage through the throat—one can imagine a gravitational analog of transition radiation but that involves details of the exotic matter we are not considering here.

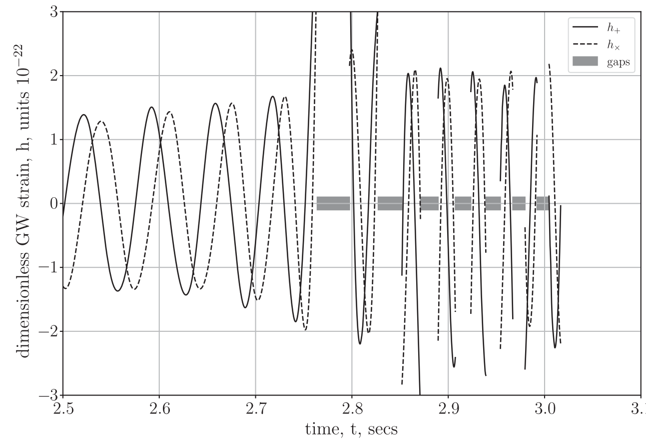

FIG. 5. Shown here is the dimensionless gravitational strain of Fig. 4 showing the gaps at the late times when the BH is passing back and forth between universes. We display only waves for Universe 1.

We assumed a distance of 500 Mpc and an inclination of the binary orbital plane of $\varphi = \theta = \pi/4$. Both polarizations are shown in Fig. 4, with plus polarization h_+ shown as solid, and the cross polarization $h_\times$ as dashed. One finds the inspiral to have a frequency of approximately 9 Hz near $t = 0$. This is in the frequency band anticipated for future 3-G detectors [58]. This scales inversely with the total mass, so a less massive system could be at high enough frequency to be observed by LIGO and a more massive system could be observable with Laser Interferometer Space Antenna. We estimate the signal to noise for the waveform in Fig. 4, with sky and polarization averaging [57] to be ∼6 for Advanced-LIGO and ∼400 for the third-generation GW detector Cosmic Explorer [59,60]. In the figures, we use gray bars to emphasize the gaps in the GW waveform. Generically, one can see that for a WH, a somewhat normal inspiral occurs and is reflected in the GW signature. However, the BH does not merge but passes through the throat, creating a gap in the waveform earlier than if a merger took place. In the case shown, the inspiral is followed by roughly half-cycle bursts of GWs of slowly decreasing amplitude. It should be noted that the gap appearing at $t \sim 2.8$ s could contain additional signals if one includes the echoes from scattering off of the wormhole geometry [11,12].

We can compare our findings with the results from authors who have considered echoes from mergers with compact objects other than BHs, since our wormholes appear compact in both Universe 1 and 2 with a δ shell of exotic matter at $R = 3M$. To estimate the error we are making by ignoring possible echoes off a dynamical δ shell, we will compare with the gravastar [61] echoes obtained by [33,34] and expect other cases to be qualitatively similar.

Pani *et al.* [33,34] have made a detailed study of particles orbiting a δ-shell gravastar (GS). They treat the δ shell as dynamical which, when excited, leads to GW echoes. What they find is that these signals can be large if quasinormal modes are excited, but this takes place for only a small number of mode frequencies depending on the compactness parameter $\mu = M/a$, where M is the apparent mass of the GS and a is the radius of the δ shell. For the GS, the resonances are confined to the region $1/4 \leq \mu$. The WHs we study have $\mu = 1/3$ and are hence outside this region. Comparing with a GS at $\mu = 1/3$ though, we see the corrections to the Schwarzschild BH are small and of order $\leq 2\%$. (See Fig. 2 of [34].) We expect this to be roughly the case in general for other objects with structure outside the horizon at $\mu = 1/2$ until the resonance region is reached, and for the WH case in particular. Hence, we expect only a few percent correction from echoes relative to the results we display. We caution that WHs constructed differently, for example with multiple δ shells, could potentially have more complex signatures including echoes, but this is outside the scope of the present work.

IV. SUMMARY AND DISCUSSION

Gravitational wave astronomy will continue to expand its sensitivity, eventually producing a census of massive binary inspirals extending to high redshifts that could encompass even the first generation of seed BH-BH mergers [e.g. [62,63]]. With this increased sensitivity, the possibility of constraining (or detecting!) exotic phenomena via GW signals has arrived. In the present work, we have examined a novel antichirp signature arising from a bound binary traversable WH system, where the bound object emerges through the wormhole throat into our region of spacetime. Since the WH throat is at a larger radius than the event horizon of a BH of the same mass, a WH-BH interaction would be *distinguishable* even during an inspiral, because the signal would drop off at a lower frequency than is expected for the same mass BH-BH merger. After the initial inspiral, we expect the spikes at the exotic matter boundary to be strong and unique, though it requires a model of the exotic matter and black hole interaction to further explore this. One can imagine phenomena in the motion of the exotic matter as the BH traverses it that would give rise to strong GWs, a sort of gravitational transition radiation. Finally, if there is no ringdown GW merger signal, then this would also be evidence for something other than a BH-BH merger.

We have been assuming near-circular orbits for BHs near WHs, but this does not always have to be the case. For example, Kozai [42] and Lidov [43] have shown that three body effects can give nonzero eccentricities to orbits that are initially circular. Thus, even though binary orbits tend to circularize due to the effects of GW radiation, if there is another body in the vicinity, the Kozai-Lidov mechanism could lead to an orbit that is eccentric as a BH crosses a WH throat. Overall this would imply a higher chance of orbits where the BH starting in Universe 1 either escapes into Universe 2 or starts off with an eccentric bound orbit in Universe 2. This is just one example of beyond circular orbit signal possibilities one could expect for BH-WH encounters.

Although we are by no means WH advocates, WHs have been offered as plausible explanations in astronomy. They have been suggested as possible sources of fast radio bursts [64] and the LIGO-VIRGO event GW190521 [65]. They also provide another form of compact object as an alternative to a supermassive BH, e.g., as the only other possibility for Sgr A^* consistent with the observed orbits of S stars[66]. Their discovery could imply the possible existence of exotic matter [17,18,67]—though WHs in a modified gravity scenario are possible without exotic matter [68,69] as well. WHs would also allow shortcuts through our Universe which have implications for cosmology [70] and beyond.

This initial work posits the unique gravitational signature of a potential WH-BH interaction, but it merely scratches the surface of this domain. For example, we considered a Schwarzschild-like traversable WH with a simplified choice of exotic matter, but a spinning WH solution may be more astrophysically relevant. In addition to mapping eccentric orbits, future avenues include the effect of higher-order modes on the outspiral waveforms; astrophysical implications of WH-BH binaries, which can constrain WH demographics; interactions of BHs or matter with the exotic matter that can lead to strong GWs; and potential multimessenger signals of WH-BH systems.

To reiterate: the purpose of the current work has been to demonstrate potential novel features of a WH-BH interaction not yet discussed in the literature, rather than give a detailed calculation. The prevalence of unknowns, from the interaction properties of the matter on the throat, to the structure of the throat itself (i.e. can it vary from a δ shell), provide tremendous opportunities for further extensions and refinements of the present work, and are currently under study.

ACKNOWLEDGMENTS

The work of T. W. K. is supported by U.S. DoE Grant No. DE-SC-0019235. J. B. D. acknowledges support from the National Science Foundation under Grant No. NSF PHY-1820801. J. B.D would also like to thank the Mitchell Institute for Fundamental Physics and Astronomy at Texas A&M University for their generous hospitality during various stages of this work. The authors would like to thank Dr. Karan Jani for valuable discussions.

[1] B. P. Abbott *et al.* (LIGO Scientific and Virgo Collaborations), Phys. Rev. Lett. **116**, 061102 (2016).
[2] B. P. Abbott *et al.* (LIGO Scientific and Virgo Collaborations), Phys. Rev. Lett. **119**, 161101 (2017).
[3] B. P. Abbott *et al.* (LIGO Scientific and Virgo Collaborations), Astrophys. J. Lett. **892**, L3 (2020).
[4] B. P. Abbott *et al.* (LIGO Scientific and Virgo Collaborations), Phys. Rev. X **9**, 031040 (2019).
[5] A. Vilenkin and E. P. S. Shellard, *Cosmic Strings and Other Topological Defects* (Cambridge University Press, Cambridge, England, 2000).
[6] K. W. K. Wong, E. Berti, W. E. Gabella, and K. Holley-Bockelmann, Mon. Not. R. Astron. Soc. **483**, L33 (2019).
[7] J. A. Wheeler, Phys. Rev. **97**, 511 (1955).
[8] J. Wheeler, *Geometrodynamics* (Academic Press, New York, 1962).
[9] V. Cardoso, E. Franzin, and P. Pani, Phys. Rev. Lett. **116**, 171101 (2016); **117**, 089902(E) (2016).
[10] V. Cardoso, S. Hopper, C. F. B. Macedo, C. Palenzuela, and P. Pani, Phys. Rev. D **94**, 084031 (2016).
[11] Z. Mark, A. Zimmerman, S. M. Du, and Y. Chen, Phys. Rev. D **96**, 084002 (2017).
[12] P. Bueno, P. A. Cano, F. Goelen, T. Hertog, and B. Vercnocke, Phys. Rev. D **97**, 024040 (2018).
[13] S. Aneesh, S. Bose, and S. Kar, Phys. Rev. D **97**, 124004 (2018).
[14] J. Abedi and N. Afshordi, J. Cosmol. Astropart. Phys. 11 (2019) 010.
[15] J. Abedi and N. Afshordi, arXiv:2001.00821.
[16] A. A. Kirillov, E. P. Savelova, and O. M. Lecian, arXiv:2003.13127.
[17] M. S. Morris and K. S. Thorne, Am. J. Phys. **56**, 395 (1988).
[18] M. S. Morris, K. S. Thorne, and U. Yurtsever, Phys. Rev. Lett. **61**, 1446 (1988).
[19] M. Visser, *Lorentzian Wormholes: From Einstein to Hawking* (AIP Press, Woodbury, NY, 1995).
[20] M. Visser, Nucl. Phys. **B328**, 203 (1989).
[21] M. Visser, Phys. Lett. B **242**, 24 (1990).
[22] R. L. Arnowitt, S. Deser, and C. W. Misner, Gen. Relativ. Gravit. **40**, 1997 (2008).
[23] W. Israel, Nuovo Cimento B **44**, 1 (1966); **48**, 463(E) (1967).
[24] S. W. Hawking and G. F. R. Ellis, *The Large Scale Structure of Space-Time*, Cambridge Monographs on Mathematical Physics (Cambridge University Press, Cambridge, England, 2011).
[25] R. V. Buniy and S. D. H. Hsu, Phys. Lett. B **632**, 543 (2006).
[26] R. V. Buniy, S. D. H. Hsu, and B. M. Murray, Phys. Rev. D **74**, 063518 (2006).
[27] E. Poisson and M. Visser, Phys. Rev. D **52**, 7318 (1995).
[28] V. Varela, Phys. Rev. D **92**, 044002 (2015).
[29] L. Ford and T. A. Roman, Phys. Rev. D **51**, 4277 (1995).
[30] A. Borde, L. Ford, and T. A. Roman, Phys. Rev. D **65**, 084002 (2002).
[31] L. Ford, A. D. Helfer, and T. A. Roman, Phys. Rev. D **66**, 124012 (2002).
[32] M. Visser, S. Kar, and N. Dadhich, Phys. Rev. Lett. **90**, 201102 (2003).
[33] P. Pani, E. Berti, V. Cardoso, Y. Chen, and R. Norte, Phys. Rev. D **80**, 124047 (2009).
[34] P. Pani, E. Berti, V. Cardoso, Y. Chen, and R. Norte, Phys. Rev. D **81**, 084011 (2010).
[35] C. Molina, P. Pani, V. Cardoso, and L. Gualtieri, Phys. Rev. D **81**, 124021 (2010).
[36] K. Glampedakis and D. Kennefick, Phys. Rev. D **66**, 044002 (2002).
[37] A. Arvanitaki, M. Baryakhtar, and X. Huang, Phys. Rev. D **91**, 084011 (2015).
[38] R. Brito, S. Ghosh, E. Barausse, E. Berti, V. Cardoso, I. Dvorkin, A. Klein, and P. Pani, Phys. Rev. Lett. **119**, 131101 (2017).
[39] S. Ghosh, E. Berti, R. Brito, and M. Richartz, Phys. Rev. D **99**, 104030 (2019).
[40] S. Ghosh, Gravitational radiation from superradiant instabilities of rotating black holes, Ph.D. thesis, University of Mississippi, USA, 2019.
[41] L. Blanchet, Living Rev. Relativity **17**, 2 (2014).
[42] Y. Kozai, Astron. J. **67**, 591 (1962).
[43] M. L. Lidov, Planet. Space Sci. **9**, 719 (1962).
[44] It is an open question if these exist when GWs are considered.
[45] V. Diemer and E. Smolarek, Classical Quantum Gravity **30**, 175014 (2013).
[46] S. Mikkola and D. Merritt, Mon. Not. R. Astron. Soc. **372**, 219 (2006).
[47] S. Mikkola and D. Merritt, Astron. J. **135**, 2398 (2008).
[48] L. Blanchet, S. Detweiler, A. Le Tiec, and B. F. Whiting, Phys. Rev. D **81**, 064004 (2010).
[49] C. M. Will, Proc. Natl. Acad. Sci. U.S.A. **108**, 5938 (2011).
[50] S. Borhanian, K. G. Arun, H. P. Pfeiffer, and B. S. Sathyaprakash, Classical Quantum Gravity **37**, 065006 (2020).
[51] M. Boyle, D. A. Brown, L. E. Kidder, A. H. Mroué, H. P. Pfeiffer, M. A. Scheel, G. B. Cook, and S. A. Teukolsky, Phys. Rev. D **76**, 124038 (2007).
[52] C. O. Lousto and J. Healy, Phys. Rev. Lett. **125**, 191102 (2020).
[53] C. O. Lousto and Y. Zlochower, Phys. Rev. Lett. **106**, 041101 (2011).
[54] S. Husa, S. Khan, M. Hannam, M. Pürrer, F. Ohme, X. J. Forteza, and A. Bohé, Phys. Rev. D **93**, 044006 (2016).
[55] K. Jani, J. Healy, J. A. Clark, L. London, P. Laguna, and D. Shoemaker, Classical Quantum Gravity **33**, 204001 (2016).
[56] M. van de Meent and H. P. Pfeiffer, Phys. Rev. Lett. **125**, 181101 (2020).
[57] M. Maggiore, *Gravitational Waves: Volume 1: Theory and Experiments* (OUP Oxford, New York, 2008).
[58] GWIC, Gravitational-wave astronomy with the next-generation earth-based observatories (2019).
[59] D. Reitze *et al.*, Bull. Am. Astron. Soc. **51**, 035 (2019), arXiv:1907.04833.
[60] Cosmic explorer website, https://cosmicexplorer.org, accessed: 2020-07-09.
[61] P. O. Mazur and E. Mottola, arXiv:gr-qc/0109035.
[62] H. Yu *et al.*, Phys. Rev. Lett. **120**, 141102 (2018).
[63] M. Colpi, K. Holley-Bockelmann, T. Bogdanovic, P. Natarajan, J. Bellovary, A. Sesana, M. Tremmel, J. Schnittman, J. Comerford, E. Barausse, E. Berti, M. Volonteri, F. Khan, S. McWilliams, S. Burke-Spolaor, J.

Hazboun, J. Conklin, G. Mueller, and S. Larson, arXiv:1903.06867.
[64] D. F. Torres, G. E. Romero, and L. A. Anchordoqui, Phys. Rev. D **58**, 123001 (1998).
[65] M. J. Graham *et al.*, Phys. Rev. Lett. **124**, 251102 (2020).
[66] D.-C. Dai and D. Stojkovic, Phys. Rev. D **100**, 083513 (2019).
[67] D. Hochberg and T. W. Kephart, Phys. Lett. B **268**, 377 (1991).
[68] F. Duplessis and D. A. Easson, Phys. Rev. D **92**, 043516 (2015).
[69] J. B. Dent, D. A. Easson, T. W. Kephart, and S. C. White, Int. J. Mod. Phys. D **26**, 1750117 (2017).
[70] D. Hochberg and T. W. Kephart, Phys. Rev. Lett. **70**, 2665 (1993).